# 50-Hertz Magnetic Field and Calcium Transients in Jurkat Cells: Results of a Research and Public Information Dissemination (RAPID) Program Study

***Howard E. Wey,* David P. Conover, Patty Mathias, Mark Toraason, and W. Greg Lotz***

The National Institute for Occupational Safety and Health, Cincinnati, Ohio, USA

An effect on intracellular calcium continues to be proposed as a biochemical pathway for the mediation of biologic effects of electrical-power-frequency magnetic fields (MF). However, reproducible results among laboratories are difficult to attain and the characteristics of magnetic field effects on intracellular free calcium ($[Ca^{2+}]_i$) are not well understood. We attempted to repeat the studies of Lindström et al. [Intracellular Calcium Oscillations in a T-Cell Line by a Weak 50 Hz Magnetic Field. J Cell Physiol 156:395–398 (1993)] by investigating the effect of a 1.5-G 50-Hz MF on $[Ca^{2+}]_i$ in the Jurkat lymphocyte T-cell line. Changes in $[Ca^{2+}]_i$ were determined using microscopic imaging of fura-2 loaded Jurkat cells on poly-L-lysine-coated glass coverslips. The MF was generated by a single coil constructed with bifilar wire and located in the same plane as the cells. Cells were randomly exposed for 8 min to MF, sham field (SF), or no field (NF) conditions. The exposure condition remained coded until data analysis was complete. Each exposure period was preceded by an 8-min data collection to establish a baseline for $[Ca^{2+}]_i$. After each exposure condition, cells were exposed to anti-CD3 antibody that induced a rapid increase in $[Ca^{2+}]_i$ in responsive cells; this provided a positive control. $[Ca^{2+}]_i$ was analyzed for individual cells as spatially-averaged background-corrected 340/380 nm ratios, and a $[Ca^{2+}]_i$ transient was considered significant for positive deviations from baseline of 3× an estimate of noise in the baseline. Typically, 25–50 cells/field were viewed and approximately 50% had no $[Ca^{2+}]_i$ transients in the baseline period and also responded to positive control. Only cells responding to positive control and lacking changes in $[Ca^{2+}]_i$ during the baseline period were considered qualified for assessment during the exposure period. The incidences of $[Ca^{2+}]_i$ transients during the exposure period for two experiments (40× objective) were 16.5, 14.6, and 14.2% for MF, SF, and NF, respectively, and were not statistically significantly different. Previous studies by Lindström et al. [Intracellular Calcium Oscillations in a T-Cell Line after Exposure to Extremely-Low-Frequency Magnetic Fields with Variable Frequencies and Flux Densities. Bioelectromagnetics 16:41–47 (1995)] showed a high response rate (92%) for exposure to 1.5-G 50-Hz MF when individual cells were preselected for investigation. We found no such effect when examining many cells simultaneously in a random and blind fashion. These results do not preclude an effect of MF on $[Ca^{2+}]_i$, but suggest that responsive cells, if they exist, were not identified using the approaches that we used in this study. *Key words*: fura 2, intracellular calcium, Jurkat cells, lymphocytes, magnetic fields. *Environ Health Perspect* 108:135–140 (2000). [Online 7 January 2000]
*http://ehpnet1.niehs.nih.gov/docs/2000/108p135-140wey/abstract.html*

The reported association between exposure to magnetic fields (MF) and a variety of adverse health effects (*1,2*) has led to repeated attempts to define possible mechanisms (*3*). Calcium biochemistry has been a central focus of many of the studies because calcium is a ubiquitous second messenger in cell processes and is, in many cases, regulated at cell membranes, a purported target of MF. Over the past two decades, research using diverse *in vitro* models has demonstrated the ability of MF exposure to modify calcium metabolism, presumably by affecting calcium flux across membranes (*4–10*). However, several investigations have not detected an effect of MF on calcium metabolism or flux in a variety of cell types (*11–15*). This apparent lack of consistency among investigating groups on the effects of MF on cellular calcium mobilization has been reflected throughout the field of research into the biologic effects of MF (*16*).

Explanations for the conflicting results have invoked physical complexities related to MF exposure, biologic complexities related to heterogeneity of biologic response, or the need to establish a responsive biologic state in cells (*6,12,17–23*). Physical complexities of MF exposure are demonstrated by reports of alternating current (AC)–direct current (DC) MF interactions, frequency windows, and the dependence of effects on both frequency (AC fields) and flux density. In the case of biologic complexity associated with calcium metabolism, Walleczek and Liburdy (*24*) reported that calcium uptake in rat lymphocytes was increased by brief exposures to 60-Hz MF only in cells stimulated with the mitogen concanavalin A (ConA). In this study, those lymphocytes least responsive to ConA exhibited the greatest response to MF. In a follow-up study, Liburdy (*22*) reported that the age of the rats from which the cells were harvested also contributed to a variation in calcium response to MF.

In 1993, Lindström et al. (*25*) published the first in a series of experiments (*26–28*) that demonstrated, in real time, MF-induced changes in intracellular free calcium $[Ca^{2+}]_i$. Using the intracellular calcium probe fura-2 and fluorescence microscopy, they demonstrated that $[Ca^{2+}]_i$ transients occurred within individual Jurkat cells when the MF was present and rapidly subsided when the MF was turned off. Additionally, $[Ca^{2+}]_i$ transients in cells within the same culture could be restimulated with the reintroduction of MF. The studies of Lindström et al. (*25–27*) stand out because the investigators did not change the experimental model or exposure regimen, repeated their work, and expanded on original findings to further define the association between MF and perturbations of $[Ca^{2+}]_i$. Because of these factors, investigators at the National Institute of Occupational Safety and Health (Cincinnati, OH) elected to repeat the studies of Lindström et al. (*25–27*) in an independent laboratory.

## Materials and Methods

***Cell culture.*** We obtained the Jurkat cell line (clone E6-1), derived from a human T-cell leukemia, from E. Lindström (Umea University, Umea, Sweden). The cells were shipped as a cell suspension in RPMI-1640 (Life Technologies, Grand Island, NY) containing 10% fetal bovine serum (Hyclone, Logan, UT) in a sealed flask. The cell suspension was aliquoted into flasks at 30 mL suspension/75 $cm^2$ growing surface. The viability was initially low (approximately 30% by trypan blue exclusion), but reached 98% after 1 week in culture. The cells were grown

Address correspondence to M. Toraason, National Institute for Occupational Safety and Health (NIOSH), MS-C23, 4676 Columbia Parkway, Cincinnati OH 45226 USA. Telephone: (513) 533-8207. Fax: (513) 533-8138. E-mail: mht1@cdc.gov

*Current address: South Dakota State University, Brookings, SD 57007 USA.

We thank G. Boorman, G. Leikauf, R. Liburdy, D. Lyle, E. Lindström, M. Misakian, J. Putney, R. Savage, J. Snawder, and J. Walleczek for their recommendations and comments during the planning of this research and/or the writing of this report.

This study was supported by the National Institute of Environmental Health Sciences and NIOSH under Interagency Agreement no. YOI-ES-50313 to meet the goals of the electric and magnetic fields Research and Public Information Dissemination Program.

Received 4 March 1999; accepted 23 August 1999.

in RPMI-1640 containing 10% fetal bovine serum (hereafter called complete medium), and maintained in a Forma incubator (Forma Scientific, Inc., Marietta, OH) at 37°C with a humidified atmosphere of 95% air and 5% $CO_2$. In the incubator with mu metal shielding (Amuneal Manufacturing Corp., Philadelphia, PA), the maximum AC and DC magnetic flux densities were 1.4 and 7 mG, respectively. These flux densities were measured with a MultiWave II monitor (Electric Research and Management, Inc., State College, PA). The culture was diluted to $1 \times 10^5$ cells/mL complete medium every 2–3 days to maintain cell density below $2 \times 10^6$ cells/mL. Treatment for mycoplasma contamination was initially performed by adding 5 µg/mL 4-oxo-quinoline-3-carboxylic acid derivative (ICN, Costa Mesa, CA) to complete medium for 7 days. Tests for mycoplasma contamination were routinely performed using an immunocytochemical test kit (ICN). Stocks of low passage cells (a passage is defined as a dilution; thus, there are three passages/week) were frozen in liquid nitrogen and used for all experiments.

***Intracellular calcium measurements.*** We determined intracellular calcium through changes in fluorescence of the ratiometric dye fura-2 using a fluorescence microscopy imaging system. Jurkat cells were simultaneously loaded with fura-2 and immobilized on poly-L-lysine (PLL)-coated glass coverslips (25 mm Fisherbrand, catalog no. 12-545-102; Fisher Scientific, Inc., Pittsburgh, PA). One side of the glass coverslips was coated with PLL by placing them on the surface of a 0.01% solution of PLL in sterile water for 30 sec. Excess liquid was drained by touching the edge of the coverslip with tissue. Coverslips were allowed to air dry before being placed individually, coated-side up, in 35-mm tissue culture dishes. For plating on coverslips, Jurkat cell suspension in complete medium was diluted 1:1 with Krebs-Hepes buffer containing 1% bovine serum albumin (KHB) and an aliquot of fura-2/AM (Molecular Probes, Eugene, OR) added to a final concentration of 2 µM, and a 200-µL aliquot was placed on top of the PLL-coated glass coverslip. The coverslip cultures were incubated at 37°C in a humidified atmosphere of 95% air and 5% $CO_2$ for 60 min. KHB (2 mL) was then carefully added to the culture dish containing the Jurkat coverslip culture. The coverslip was removed with forceps, dipped in KHB, mounted in a holder, and the culture covered with KHB (0.5 mL, 37°C). The coverslip holder containing the culture was immediately mounted in the exposure chamber on the microscope stage and suffusion with KHB (37°C) at 0.6 mL/min was started. The cells were illuminated briefly as the fluorescent image was brought into focus and the intensifier gain adjusted such that the pixel values for cell fluorescence were in the middle of the dynamic range for both 380 and 340 nm excitation. The process of mounting the culture caused $[Ca^{2+}]_i$ transients, which subsided after 20 min. Thus, cells were kept in the dark for approximately 20 min before the start of an experiment.

Instrument control and data acquisition were facilitated by a personal computer-based image analysis system (MetaFluor; Universal Imaging Corp., West Chester, PA). The excitation source was a 75-W xenon lamp. Wavelength selection was accomplished using bandpass filters (340HT15 or 380HT15 from Omega Optical, Brattleboro, VT) mounted in a 10-position filter wheel (Sutter Instrument Company, Novato, CA). Neutral density filters were mounted together with the bandpass filters, as needed, to balance light intensity at 340 and 380 nm excitation. The position and movement of the filter wheel were controlled by the imaging software, and were integrated with data collection. All excitation light also passed through an additional neutral density filter to reduce light intensity, and through an infrared absorption filter to minimize localized sample heating. The xenon lamp and filter wheel were mounted on a Nikon Diaphot inverted epifluorescence microscope (Nikon, Inc., Melville, NY) equipped with a variety of low ultraviolet (UV)-absorbing objectives (20×, 40×, and 100×) and a filter cube containing a 400-nm dichroic mirror and a 515-nm barrier filter. Fluorescence was detected by an intensified charge-coupled device camera (DAGE/MTI CCD72; DAGE-MTI, Inc., Michigan City, IN) and subsequently digitized by the image analysis system.

Fluorescence data were collected and saved as image sets every 2–2.5 sec and subsequently analyzed to determine $[Ca^{2+}]_i$ (Figure 1). Each image set contained 340 and 380 nm excitation data. A circular target area was established around all qualified cells using the first image of an experiment and was applied to every image set in an experiment. Qualified cells included all cells that did not exhibit $[Ca^{2+}]_i$ transients in the initial baseline period and responded to the positive control (anti-CD3 antibody). Targets were only created around fully visible cells that were not in contact with other cells. Small circular targets were also created in background space adjacent to targeted cells for the collection of background fluorescence. At each image set the average pixel value for a background target was subtracted from the average pixel value for the corresponding cell target. We were only interested in detecting the presence of $[Ca^{2+}]_i$ transients as defined by a significant change in $[Ca^{2+}]_i$ above a stable baseline. Therefore, a calibration procedure was not performed, and the ratio of fluorescence at 340 to 380 nm excitation was used as a measure of $[Ca^{2+}]_i$.

***Magnetic field exposure.*** The MF exposure chamber was custom machined from an aluminum block. The exposure chamber was open in the center and secured the coverslip holder in place over the microscope objective. A commercially available coverslip holder (Leiden open perfusion chamber; Medical Systems Corp., Greenvale, NY) was modified by the replacement of the stainless steel base with an aluminum base. The top of the coverslip holder was made of Teflon with rubber O-rings. A plexiglass cover over the top of the coverslip holder secured entry and exit tubing for the suffusion of cells with buffers. A thin 3.2-cm coil was located in a circular groove surrounding the coverslip holder and was in the same plane as the coverslip. Current flow was produced by a Hewlett-Packard 8904A signal generator (Hewlett-Packard, Palo Alto, CA) and a Techron 5515 power amplifier (Techron, Elkhart, IN). The coil operated at 50 Hz and produced a 1.5-G field over an exposure volume of 1 $cm^3$. The coil contained bifilar magnet wire custom-wound to allow either active field cancellation (sham exposure) or applied field generation. A cross-over switch with positions labeled "A" and "B" was used to set MF and sham field (SF) conditions. In addition, a second switch labeled "C" and "D" was used for no current flow (no field; NF) or current flow for MF or SF conditions. In the

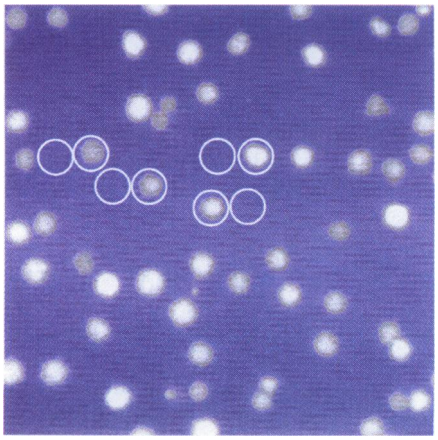

**Figure 1.** Pseudocolor fluorescent image of fura 2-loaded Jurkat cells under a 40× objective. At the onset of each experiment, Jurkat cells were selected for inclusion in an experiment by establishing a circular target around each qualified cell using image analysis software. A circular target adjacent to the selected cells was used for background subtraction. For illustration purposes, only four cells have been selected; normally, approximately 40 cells would be selected from a field comparable to that in the figure. $[Ca^{2+}]_i$ was continuously monitored in cells using ratiometric analysis. Magnification ×140.

NF condition, current flowed only through a dummy coil that was remotely located from the exposure volume. This arrangement ensured that the experimenter was blind to the field conditions. MF conditions were measured with a Multiwave II monitor. In addition, we measured the DC and AC MF perturbation (orientation, strength) from our objectives with a gauss meter (MNA-1904-VH and MNT-4E04-VH probes and 450 meter; Lake Shore Cryotonics, Inc., Westerville, OH). At the cell location, the maximum DC perturbation was 23, 26, and 22 mG (with no changes in field direction) for the 20×, 40×, and 100× objectives, respectively. The DC magnetic flux density was 491 mG in the absence of objectives. The AC magnetic flux densities were perturbed 1.7, 0.2, and 0.6% by the 20×, 40×, and 100× objectives, respectively.

***Temperature control.*** The temperature of the buffer in direct contact with the cells was maintained within a small range. For any given experiment, the mean temperature of the buffer in contact with cells was between 36.5 and 37.0°C with a standard deviation around the mean not exceeding 0.08°C. A plexiglass box (Nikon) enclosed the microscope stage, objective, condenser, and filter cube. Air temperature within the box was controlled by an air heater-controller (Air-Therm; World Precision Instruments, Sarasota, FL) with a thermocouple placed in a slot in the aluminum exposure chamber. This arrangement maintained the aluminum exposure chamber on the microscope stage at a set temperature of 37°C. The suffusate buffer was warmed by running though tubing contained in a water jacket. The temperature of the water jacket was maintained by a circulating water bath (Lauda M3, Lauda-Konigshofen, Germany). The temperature of the buffer in the cell holder was continuously monitored with a YSI451 temperature probe (Yellow Springs Instruments, Yellow Springs, OH) and meter (model H-08502-16; Cole-Palmer Instrument Co., Vernon Hills, IL).

***Experimental procedure and data analysis.*** All experiments were blind. Two switches were used to set the field condition, as described in "Magnetic Field Exposure." Experiments were performed in a randomized block design, and all exposure conditions were performed in random order once each day. In their first publication, Lindström et al. (*25*) collected fluorescence data from experiments that lasted 16 min. We followed the same design with the modification that data were collected for an additional 6 min to include exposure to a positive control (anti-CD3 antibody). For each experiment, we obtained a baseline in the first 8 min, followed by MF, SF, or NF conditions for an additional 8 min. Finally, cells were exposed to anti-CD3 antibody (0.5 µg/mL) for 6 min.

Lindström et al. (*25–27*) used a photomultiplier tube for fluorescence detection. Use of the tube allowed data to be collected from only one cell at a time. This approach also necessitated the use of selection criteria for choosing a cell for study before MF exposure. Primary criteria were the general morphology of the cell, the absence of spontaneous calcium transients within a 5-min observation period, the absence of cell–cell contact, and a low basal calcium level. The use of fluorescence imaging enabled data collection from a field of cells simultaneously and eliminated the need to impose subjective selection criteria before MF exposure. The response of cells during each period was determined as yes (Y) or no (N) for the presence of $[Ca^{2+}]_i$ transients. $[Ca^{2+}]_i$ transients were identified as the $F_{340}/F_{380}$ ratio exceeding 3 × an estimate of baseline noise for 5 consecutive data points (10 sec). An estimate of baseline noise was calculated as 2 SD of the average $F_{340}/F_{380}$ ratio during baseline regions in the first 8 min. The incidence of $[Ca^{2+}]_i$ transients in the exposure period was calculated as NYY/(NYY + NNY), where N represents no $[Ca^{2+}]_i$ transients and Y represents the presence of $[Ca^{2+}]_i$ transients in the preexposure (baseline), exposure (NF, SF, or MF), or postexposure (positive control) periods. For example, no $[Ca^{2+}]_i$ transients during baseline and $[Ca^{2+}]_i$ transients present during the exposure and positive control periods would be expressed as NYY (Figure 2). The incidence of responders in the presence of MF was compared to the incidence of responders in the absence of MF (SF and NF groups) by analysis of variance using a randomized block design. To qualify for analysis, cells could not exhibit $[Ca^{2+}]_i$ transients during the preexposure baseline period and had to exhibit $[Ca^{2+}]_i$ transients during the postexposure positive control period. For cells meeting these criteria, a score of NNY was given for no $[Ca^{2+}]_i$ transient in the exposure period, and a score of NYY was given for cells with $[Ca^{2+}]_i$ transients in the exposure period.

## Results

Only cells that responded to positive control and that lacked changes in $[Ca^{2+}]_i$ during the baseline period were scored as responders or nonresponders to MF depending on their response during the exposure period. Examples of $[Ca^{2+}]_i$ responses in qualified cells are illustrated in Figure 2B, C. Three experiments were performed: two with a 40× objective and one with a 20× objective (Table 1). Of the experiments with a 40× objective, the first included eight sets of MF, SF, and NF conditions, and the second included seven sets of MF, SF, and NF conditions. For the experiment with the 20× objective, five sets of MF, SF, and NF conditions were performed (Table 1). There were no differences between any of the exposure conditions in the percentage of cells disqualified because of a preexposure response or a lack of response to anti-CD3 (Table 1). However, the preexposure response of a cell preparation was a predictor of the incidence of $[Ca]_i$ transients during the exposure period. This is shown in Figure 3 as a positive correlation between the preexposure response and the response during the exposure period, and could be interpreted as an influence of "culture excitability" on the occurrence of $[Ca]_i$ transients during the exposure period. The influence of preexposure response appeared to only be an issue for experiments using the 40× objective because, as shown in Figure 3, the incidence of spontaneous $[Ca^{2+}]_i$ transients was consistently lower for experiments using the 20× as compared to the 40× objective. To account for this relationship in the data analysis of experiments 1 and 2 (40×), the preexposure response was included in the analysis of variance model as a covariate. For all three experiments, the incidence of $[Ca^{2+}]_i$ transients in the exposure period, expressed as percent qualified cells that exhibited a $[Ca^{2+}]_i$ transient, was not different in the presence of a 50-Hz 1.5-G MF than for NF or SF conditions (Table 1).

Lindström et al. (*26*) generally observed cells for 4 min MF exposure and found that $[Ca^{2+}]_i$ transients were initiated within

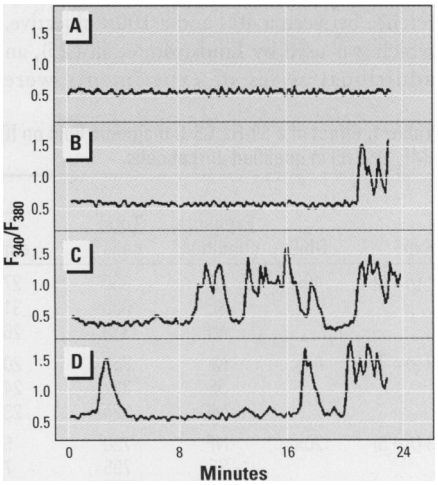


**Figure 2.** Four examples of $[Ca^{2+}]_i$ profiles from the eight possible outcomes of an experiment. The baseline or preexposure period was from 0 to 8 min. The exposure period (when NF, SF, or MF was applied) was from 8 to 16 min. At 16 min, suffusion with 0.5 µg/mL anti-CD3 is initiated. (*A*) NNN. (*B*) NNY and (*C*) NYY are the only two outcomes that were classified as qualified cells. (*D*) YNY.

30–180 sec of the onset of MF exposure. One might expect that $[Ca^{2+}]_i$ transients in cells responsive to an MF might be temporally linked to the initiation of MF exposure. This would imply that in unexposed cultures the time to the first $[Ca^{2+}]_i$ transient would be randomly distributed across the 8-min exposure period, whereas in MF-exposed cells the first $[Ca^{2+}]_i$ transients would occur close to the start of MF exposure and result in a skewed distribution. As a consequence, the inclusion of $[Ca^{2+}]_i$ transients that occurred at any time during an 8-min period may dilute an effect of MF. We examined the incidence of $[Ca^{2+}]_i$ transients in the first 4 min of the exposure period. We did not find any consistent significant effect of MF on $[Ca^{2+}]_i$ transients, although the individual comparison of MF to NF approached statistical significance (Table 1). However, in some cases (three for NF and one for SF), reducing the observation period to 4 min resulted in no $[Ca^{2+}]_i$ transients being observed. Because the limit of detection for $[Ca^{2+}]_i$ transients with an average of 26 qualified cells was approximately 3.8%, a bias may exist in the analysis of the first 4 min because of insufficient sample size. We also determined the time to the first $[Ca^{2+}]_i$ transient for each qualified cell that exhibited a $[Ca^{2+}]_i$ transient during the exposure period. There was no significant influence of MF on the distribution of time to first $[Ca^{2+}]_i$ transient (data not shown).

The incidence of spontaneous $[Ca^{2+}]_i$ transients was consistently lower for experiments using the 20× as compared to the 40× objective. To address whether this was a significant difference and also if there was a difference between a 40× and a 100× objective, which was used by Lindström et al. (*25*), an additional series of experiments were conducted with objectives with different magnification (20×, 40×, and 100×). Experiments were performed using all objectives on the same day. These experiments only assessed the level of spontaneous $[Ca^{2+}]_i$ transients during no field conditions. The 20× objective resulted in a significantly lower incidence of spontaneous $[Ca^{2+}]_i$ transients than the 40× or 100× objectives (Table 2). There was no significant difference between the 40× and 100× objectives.

## Discussion

The objective of the present investigation was to replicate the results reported by Lindström et al. (*25*). They examined MF modulation of $[Ca^{2+}]_i$ in Jurkat cells in real time. This provided the opportunity for each cell to serve as its own control and to monitor cells before, during, and after exposure to MF. These studies demonstrated that in 80–85% of Jurkat cells examined, $[Ca^{2+}]_i$ increased shortly after the introduction of an MF and returned to preexposure levels when the field was turned off (*25–27*).

A key consideration in the identification of an effect of MF on Jurkat $[Ca^{2+}]_i$ is the ability to distinguish MF-induced $[Ca^{2+}]_i$ transients from spontaneous $[Ca^{2+}]_i$ transients. This is because a fraction of Jurkats in a population experience spontaneous $[Ca^{2+}]_i$ transients. The incidence of spontaneous $[Ca^{2+}]_i$ transients is reflected in the number of transients that occur during the 8 min of SF or NF exposure (Figure 1; Table 1). In an attempt to exclude cells with spontaneous $[Ca^{2+}]_i$ transients, any cell exhibiting a transient for the 8 min preceding field exposure was excluded from final analysis. Just as it was critical to reduce cells that were exhibiting spontaneous $[Ca^{2+}]_i$ transients, it was also important to include in the final analysis only cells that had the capacity to exhibit a $[Ca^{2+}]_i$ transient. Therefore, Jurkats were also challenged postexposure with anti-CD3 antibody to ensure that they were capable of increasing $[Ca^{2+}]_i$. Because contiguous cells may affect one another in terms of inducing $[Ca^{2+}]_i$ transients, only cells free from contact with other cells were included in the final analysis. These procedures are consistent with those reported by Lindström et al. (*25–27*). However, Lindström et al. (*25–27*) included one additional criterion: a subjective morphologic assessment in the selection of a single cell within a microscopic field that would be monitored during MF exposure. This morphologic assessment was accomplished with phase observation through a 100× objective, but was not feasible with our experimental setup and design.

In the present investigation, we exposed Jurkat cells to 50-Hz, 1.5-G MF in a attempt to replicate the findings of Lindström et al. (*26*) that this MF frequency and flux density induced an 85% incidence of cells responding with a elevation in $[Ca^{2+}]_i$. Although it was our intention to duplicate, to the extent possible, the protocol of Lindström et al. (*25*), early in our investigation we realized that the preselection of a subpopulation of acceptable cells based on morphologic considerations and personal judgment could not be duplicated in the absence of the original investigators. We also realized that this process could introduce a selection bias by either including or excluding cells with a capacity for spontaneous $[Ca^{2+}]_i$ transients. Therefore, we chose to use image analysis

**Table 1.** Effect of a 50-Hz 1.5-G magnetic field on $[Ca^{2+}]_i$ transients during the application of field conditions (MF, SF, NF) in qualified Jurkat cells.

| Exp[a] | Obj[b] | Exposure condition[c] | Total cells[d] | Disqualified (%) Pre-exposure[e] | Disqualified (%) Post-exposure[f] | $[Ca^{2+}]_i$ transients during exposure period (%)[g,h] Entire 8 min | $[Ca^{2+}]_i$ transients during exposure period (%)[g,h] First 4 min[i] |
|---|---|---|---|---|---|---|---|
| 1 ($n$ = 8) | 40× | NF | 330 | 27.2 ± 14.4 | 13.8 ± 9.9 | 16.2 ± 9.7 | 5.6 ± 5.6 |
| | | SF | 333 | 31.4 ± 10.1 | 10.4 ± 5.3 | 17.9 ± 11.6 | 10.9 ± 9.5 |
| | | MF | 319 | 26.3 ± 16.4 | 14.1 ± 4.9 | 19.4 ± 10.0 | 12.2 ± 5.8 |
| 2 ($n$ = 7) | 40× | NF | 363 | 20.8 ± 17.3 | 11.8 ± 4.5 | 11.9 ± 11.4 | 8.6 ± 8.0 |
| | | SF | 327 | 24.6 ± 12.0 | 10.2 ± 5.4 | 11.0 ± 8.0 | 5.0 ± 6.1 |
| | | MF | 324 | 23.9 ± 16.0 | 14.7 ± 9.7 | 13.2 ± 8.3 | 8.5 ± 6.7 |
| 3 ($n$ = 5) | 20× | NF | 720 | 5.9 ± 4.5 | 18.0 ± 3.6 | 3.1 ± 1.3 | 1.9 ± 1.0 |
| | | SF | 795 | 7.9 ± 4.4 | 21.0 ± 5.7 | 1.7 ± 1.9 | 1.1 ± 1.4 |
| | | MF | 791 | 5.9 ± 5.5 | 19.8 ± 5.7 | 2.2 ± 0.7 | 0.7 ± 0.9 |

Abbreviations: ANOVA, analysis of variance; exp, experiment; obj, objective.
[a]The number of replicates is given in parentheses. [b]Microscope objective magnification. [c]The MF was 50 Hz, 1.5 G (0.15 μT). [d]The number of cells exhibiting all possible responses. [e]Cells were disqualified because of a $[Ca^{2+}]_i$ transient in the preexposure period. [f]Cells were disqualified because of a lack of response to anti-CD3. [g]Percent of qualified cells that exhibited a $[Ca^{2+}]_i$ transient during the exposure period; qualified cells are defined in Figure 2. [h]Data for experiments 1 and 2 were analyzed together by ANOVA with preexposure response as a covariate. There were no statistically significant differences ($p < 0.05$) between any of the exposure conditions. Experiment 3 was analyzed separately by ANOVA, and there were no significant differences ($p < 0.05$) between any of the exposure conditions. [i]$p < 0.06$ for the comparison of NF to MF in experiments 1 and 2 combined (ANOVA with preexposure response as a covariate).

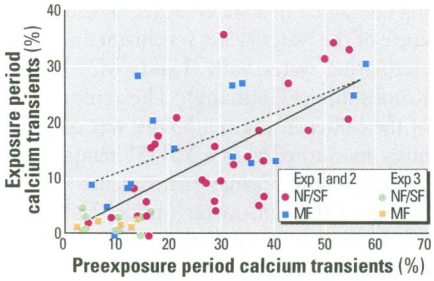


**Figure 3.** Correlation between the occurrence of $[Ca^{2+}]_i$ transients during the preexposure period and the exposure period. Exp, experiment. Only cells responding to anti-CD3 during the postexposure period were considered. The abscissa represents the percentage of cells with preexposure $[Ca^{2+}]_i$ transients; these cells were not considered (were disqualified) during the exposure period. The ordinate represents the incidence of $[Ca^{2+}]_i$ transients during the exposure period for qualified cells. We used a 40× objective in experiments 1 and 2 and a 20× objective in experiment 3. The lines drawn are from experiments 1 and 2: NF and SF combined (solid line, $R^2 = 0.45$, $p < 0.0001$); MF (dashed line, $R^2 = 0.40$, $p = 0.011$). The slope of the line for MF was not statistically significantly different ($p < 0.05$) than the slopes for NF (not shown), SF (not shown), or NF and SF combined.

and initially include all of the cells within a microscopic field. This increased the number of cells we were able to examine by > 1 order of magnitude. We also administered field conditions in random fashion and data analyses were conducted without the knowledge of the experimental field conditions. This approach avoided any potential bias that could result from the nonrandom selection of cells and exposure conditions. Using this approach, we did not find any difference in the incidence of $[Ca^{2+}]_i$ transients in cells exposed to a 50-Hz 1.5-G MF as compared to NF or to active field cancellation (SF). The results are consistent with a recent report by Lyle et al. (*15*), who used the calcium probe Fluo-3 and flow cytometry to detect MF-induced transients in Jurkats exposed to 60 Hz at approximately 0.1 mT (1 G).

Our data do not replicate the high response rate of cells to MF exposure as reported by Lindström et al. (*26*). They generally observed cells for a 4-min MF exposure and found that $[Ca^{2+}]_i$ transients were initiated within 30–80 sec of the onset of MF exposure. One might expect that $[Ca^{2+}]_i$ transients in cells responsive to an MF are temporally linked to the initiation of MF exposure. It is possible that, in unexposed cultures, the time to the first $[Ca^{2+}]_i$ transient would be randomly distributed across the 8-min exposure period, whereas in MF-exposed cells the first $[Ca^{2+}]_i$ transients would occur close to the start of MF exposure and result in a skewed distribution. As a consequence, the inclusion of $[Ca^{2+}]_i$ transients that occurred at any time during an 8-min period may dilute an effect of MF. We examined the incidence of $[Ca^{2+}]_i$ transients in the first 4 min of the exposure period. Again, no significant effect of MF on $[Ca^{2+}]_i$ transients was found (data not shown). We also determined the time to the first $[Ca^{2+}]_i$ transient for each qualified cell that exhibited a $[Ca^{2+}]_i$ transient during the exposure period. There was no significant influence of MF on the distribution of time to first $[Ca^{2+}]_i$ transient (data not shown).

Galvanovskis et al. (*29*) performed experiments comparable to those reported here and by Lindström et al. (*25*). Consistent with present observations, Galvanovskis et al. (*29*) found that 50-Hz MF did not stimulate a change in $[Ca^{2+}]_i$ in Jurkat cells with stable low-level $[Ca^{2+}]_i$. However, these authors also examined the effects of MF on cells exhibiting sustained $[Ca^{2+}]_i$ oscillations. The authors attributed the sustained oscillations to an "inhomogeneous" response to PLL, which was used, as in the present study, to secure Jurkats to cover slips. In the present investigation, cells exhibiting sustained $[Ca^{2+}]_i$ oscillations were classified as unqualified based on the original criteria of Lindström et al. (*25*) and were excluded from analysis. In the investigation of Galvanovskis et al. (*29*), visual examination of the oscillations revealed no obvious effect of MF. The authors performed power spectrum analysis on seven cells exhibiting $[Ca^{2+}]_i$ oscillations. In three of the seven cells, power-spectral density of $[Ca^{2+}]_i$ oscillations were significantly reduced during exposure to 50 Hz MF as compared to field-off conditions in the same cells. Although the results reported by Galvanovskis et al. (*29*) are intriguing, the limited number of cells evaluated requires that follow-up studies be performed for verification. There is the potential for the present data set to be evaluated for this phenomenon, but because it consists of $[Ca^{2+}]_i$ measurements on > 4,000 Jurkat cells, it will have to await an independent assessment.

Another potentially important difference between the present results and those of Lindström et al. (*25*) pertains to the type of microscope objective. We conducted our studies with both 20× and 40× objectives, whereas Lindstrom et al. (*25,26*) used a 100× objective. Too few cells were contained within the field of view at 100× (approximately 8–12) for the use of the statistical approach in the present study. On the other hand, a 100× objective provides superior assessment of morphology and therefore was the most useful method for the approach taken by Lindström et al. (*25*). Microscope objectives can perturb the MF (*30*), and the influence that this might have on the interaction with cells is not known. At the location of the cells, the maximum DC perturbation was 23, 26, and 22 mG (with no changes in field direction) for the 20×, 40×, and 100× objectives, respectively. In comparison, Liburdy (*30*) reported a maximum perturbation of 255 mG (with changes in field direction). We found a significant difference in the incidence of $[Ca^{2+}]_i$ transients between experiments performed on the same day with a 20× objective versus a 40× objective. We did not find any difference in the frequency of $[Ca^{2+}]_i$ transients in cells illuminated with a 40× objective versus a 100× objective. One possible explanation for a difference between the 20× and the 40× or 100× objectives may involve an effect of UV radiation on $[Ca^{2+}]_i$. Schieven et al. (*31*) described an energy-dependent effect of UV-B (302 nm) and UV-C (254 nm) on normal human lymphocyte $[Ca^{2+}]_i$; however, only a small effect of UV-A (365 nm) was observed. Furthermore, Ihrig et al. (*32*) reported that double flashes of 334 and 380 nm induced a $[Ca^{2+}]_i$ transient in 18% of mouse neuroblastoma cells versus 0% in cells not exposed to the double flashes. The illumination intensity for epifluorescence microscopes is proportional to the square of the numerical aperture of the objective, and generally, higher magnifications have brighter illumination fields. Thus, a 40× objective would be expected to give a larger illumination intensity than a 20× objective. By this same reasoning, a 100× objective should provide more light throughput than a 40× objective. However, we did not observe a significant difference in the incidence of spontaneous $[Ca^{2+}]_i$ transients for the latter two objectives. This could be due to other factors, such as number of lenses and types of coatings, that may further modify the light throughput.

Although it is virtually impossible to repeat every detail of an experiment, especially when investigator judgment is a factor, we set out to replicate the results of Lindström et al. (*25*). We selected an MF with the frequency (50 Hz) and flux density (1.5 G) that produced maximum results. We attempted to eliminate selection bias by including all cells that qualified for assessment based on the minimum requirements of Lindström et al. (*25*). We chose a technique that allowed us to evaluate $[Ca^{2+}]_i$ transients in hundreds of individual cells. Finally, we replicated our own experiments several times using different microscope objectives. In the end, we found no effect of MF on $[Ca^{2+}]_i$ transients in Jurkat cells nor did we arrive at a satisfactory explanation for why we were unable to replicate the results of Lindström et al. (*25*). Perhaps there is a subpopulation from what we classified as qualified cells that Lindström et al. (*25*) selected to expose and evaluate on an individual basis. Approximately 50–75% of the cells in view under a microscope objective were qualified for assessment during MF

**Table 2.** The effect of microscope objective magnification on $[Ca^{2+}]_i$ transients in Jurkat cells. The incidence of $[Ca^{2+}]_i$ transients in the exposure period (responding cells) among qualified cells.

| Objective[a] | Exposure condition | Total cells[b] | Qualified cells[c] (NNY + NYY) | Responding cells[d] (NYY) | Incidence (%)[e] |
|---|---|---|---|---|---|
| 100× (*n* = 7) | NF | 81 | 61 | 6 | 12 ± 13 |
| 40× (*n* = 3) | NF | 142 | 103 | 17 | 18 ± 1 |
| 20× (*n* = 3) | NF | 443 | 296 | 11 | 3 ± 2 |

[a]Microscope objective magnification; number of replicates in parentheses. [b]Number of cells exhibiting all possible responses. [c]Number of cells that did not exhibit a $[Ca^{2+}]_i$ transient during the preexposure period and did exhibit a $[Ca^{2+}]_i$ transient when challenged with anti-CD3 antibody during the postexposure period. [d]The number of qualified cells that exhibited a $[Ca^{2+}]_i$ transient during the exposure condition period. [e]Mean ± SD of [(number of responding cells)/(number of qualified cells)] × 100.

exposure. Of these, between 2 and 20%, depending on the magnification of objective used, exhibited $[Ca^{2+}]_i$ transients regardless of whether MF was applied. Lindström et al. (*25*) applied the same criteria for qualified cells, but were required to select a single cell based on personal judgment of adequate morphology. These individually selected cells responded to an MF 80–85% of the time with an increase in $[Ca^{2+}]_i$. This subpopulation would theoretically include the cells that we observed exhibiting $[Ca^{2+}]_i$ transients during MF field exposure, but would not include the cells that we observed exhibiting $[Ca^{2+}]_i$ transients during SF exposure. It would also not include the large proportion of cells in our study that were nonresponders during MF exposure. Until this subpopulation is defined in a way that leads to reproducible identification, we conclude, based on our present results, that a 50-Hz, 1.5-G magnetic field does not effect $[Ca^{2+}]_i$ in Jurkat cells.

## References and Notes

1. Wertheimer N, Leeper E. Electrical wiring configurations and childhood cancer. Am J Epidemiol 109:273–284 (1979).
2. London SJ, Thomas DC, Bowman JD, Sobel E, Cheng TC, Peters JM. Exposure to residential electric and magnetic fields and risk of childhood leukemia. Am J Epidemiol 134:923–937 (1991).
3. Goodman EM, Greenbaum B, Marron MT. Effects of electromagnetic fields on molecules and cells. Int Rev Cytol 158:279–338 (1995).
4. Blackman CF, Benane SG, Joines WT, Hollis MA, House DE. Calcium-ion efflux from brain tissue: power-density versus internal field-intensity dependencies at 50-MHz RF radiation. Bioelectromagnetics 1:277–283 (1980).
5. Blackman CF, Benane SG, House DE, Joines WT. Effects of ELF (1-120 Hz) and modulated (50 Hz) RF fields on the efflux of calcium ions from brain tissue in vitro. Bioelectromagnetics 6:1–11 (1985).
6. Blackman CF, Benane SG, Elliott DJ, House DE, Pollock MM. Influence of electromagnetic fields on the efflux of calcium ions from brain tissue in vitro: a three-model analysis consistent with the frequency response up to 510 Hz. Bioelectromagnetics 9:215–227 (1988).
7. Blackman CF, Benane SG, House DE. The influence of temperature during electric- and magnetic-field-induced alteration of calcium-ion release from in vitro brain tissue. Bioelectromagnetics 12:173–182 (1991).
8. Dutta SK, Ghosh B, Blackman CF. Radiofrequency radiation-induced calcium ion efflux enhancement from human and other neuroblastoma cells in culture. Bioelectromagnetics 10:197–202 (1989).
9. Lyle DB, Wang XH, Ayotte RD, Sheppard AR, Adey WR. Calcium uptake by leukemic and normal T-lymphocytes exposed to low frequency magnetic fields. Bioelectromagnetics 12:145–156 (1991).
10. Flipo D, Fournier M, Benquet C, Roux P, LeBoulaire C, Pinsky C, LaBella FS, Krzystyniak K. Increased apoptosis, changes in intracellular $Ca^{2+}$, and functional alterations in lymphocytes and macrophages after in vitro exposure to static magnetic field. J Toxicol Environ Health Part A 54:63–76 (1998).
11. Bellossi A. Lack of an effect of static magnetic field on calcium efflux from isolated chick brains. Bioelectromagnetics 7:381–386 (1986).
12. Parkinson WC, Hanks CT. Search for cyclotron resonance in cells in vitro. Bioelectromagnetics 10:129–145 (1989).
13. Garcia-Sancho J, Montero M, Alvarez J, Fonteriz RI, Sanchez A. Effects of extremely-low-frequency electromagnetic fields on ion transport in several mammalian cells. Bioelectromagnetics 15:579–588 (1994).
14. Hojevik P, Sandblom J, Galt S, Hamnerius Y. $Ca^{2+}$ ion transport through patch-clamped cells exposed to magnetic fields. Bioelectromagnetics 16:33–40 (1995).
15. Lyle DB, Fuchs TA, Casamento JP, Davis CC, Swicord ML. Intracellular calcium signaling by Jurkat T-lymphocytes exposed to a 60 Hz magnetic field. Bioelectromagnetics 18:439–445 (1997).
16. National Research Council. Possible Health Effects of Exposure to Residential Electric and Magnetic Fields. Washington, DC:National Academy Press, 1996.
17. Blackman CF, Kinney LS, House DE, Joines WT. Multiple power-density windows and their possible origin. Bioelectromagnetics 10:115–128 (1989).
18. Blanchard JP, Blackman CF. Clarification and application of an ion parametric resonance model for magnetic field interactions with biological systems. Bioelectromagnetics 15:217–238 (1994).
19. Galt S, Sandblom J, Hamnerius Y, Hojevik P, Saalman E, Norden B. Experimental search for combined AC and DC magnetic field effects on ion channels. Bioelectromagnetics 14:315–327 (1993).
20. Liburdy RP. Calcium signaling in lymphocytes and ELF fields. Evidence for an electric field metric and a site of interaction involving the calcium ion channel. FEBS Lett 301:53–59 (1992).
21. Liburdy RP, Callahan DE, Harland J, Dunham E, Sloma TR, Yaswen P. Experimental evidence for 60 Hz magnetic fields operating through the signal transduction cascade. Effects on calcium influx and c-*MYC* mRNA induction. FEBS Lett 334:301–308 (1993).
22. Liburdy RP. Cellular studies and interaction mechanisms of extremely low frequency fields. Radio Sci 30:17-203 (1995).
23. Yost MG, Liburdy RP. Time-varying and static magnetic fields act in combination to alter calcium signal transduction in the lymphocyte. FEBS Lett 296:117–122 (1992).
24. Walleczek J, Liburdy RP. Nonthermal 60 Hz sinusoidal magnetic-field exposure enhances $^{45}Ca^{2+}$ uptake in rat thymocytes: dependence on mitogen activation. FEBS Lett 271:157–160 (1990).
25. Lindström E, Lindström P, Berglund A, Hansson K, Lundgren E. Intracellular calcium oscillations in a T-cell line by a weak 50 Hz magnetic field. J Cell Physiol 156:395–398 (1993).
26. Lindström E, Lindström P, Berglund A, Lundgren E, Mild KH. Intracellular calcium oscillations in a T-cell line after exposure to extremely-low-frequency magnetic fields with variable frequencies and flux densities. Bioelectromagnetics 16:41–47 (1995).
27. Lindström E, Berglund A, Mild KH, Lindström P, Lundgren E. CD45 phosphatase in Jurkat cells is necessary for response to applied ELF magnetic fields. FEBS Lett 14:118–122 (1995).
28. Korzh-Sleptsova IL, Lindström E, Mild KH, Berglund A, Lundgren E. Low frequency MFs increased inositol 1,4,5,-triphosphate levels in the Jurkat cell line. FEBS Lett 359:151–154 (1995).
29. Galvanovskis J, Sandblom J, Bergqvist B, Galt S, Hammerius Y. The influence of 50-Hz magnetic fields on cytoplasmic $Ca^{2+}$ oscillations in human leukemia T-cells. Sci Total Environ 180:19–33 (1996).
30. Liburdy RP. Microscopic objectives perturb local DC magnetic fields: a factor in EMF microscopy studies. In: Bioelectromagnetic Society Seventeenth Annual Meeting, 18–22 June 1995, Boston, Massachusetts. Frederick, MD:Bioelectromagnetic Society, 1995;42.
31. Schieven GL, Kirihara JM, Gilliland LK, Uckun FM, Ledbetter JA. Ultraviolet radiation rapidly induces tyrosine phosphorylation and calcium signaling in lymphocytes. Mol Biol Cell 4:523–530 (1993).
32. Ihrig I, Heese C, Glaser R. Alterations of intracellular calcium concentration in mice neuroblastoma cells by electrical field and UVA. Bioelectromagnetics 18:595–597 (1997).